

# **Split-ring resonator loaded miniaturised slot for the slotted waveguide antenna stiffened structure**

*March, 2011*

*A. Prof. Kamran Ghorbani  
School of Electrical & Computer Engineering, RMIT University*

Report Documentation Page				Form Approved OMB No. 0704-0188	
Public reporting burden for the collection of information is estimated to average 1 hour per response, including the time for reviewing instructions, searching existing data sources, gathering and maintaining the data needed, and completing and reviewing the collection of information. Send comments regarding this burden estimate or any other aspect of this collection of information, including suggestions for reducing this burden, to Washington Headquarters Services, Directorate for Information Operations and Reports, 1215 Jefferson Davis Highway, Suite 1204, Arlington VA 22202-4302. Respondents should be aware that notwithstanding any other provision of law, no person shall be subject to a penalty for failing to comply with a collection of information if it does not display a currently valid OMB control number.					
1. REPORT DATE <b>12 AUG 2011</b>		2. REPORT TYPE		3. DATES COVERED	
4. TITLE AND SUBTITLE <b>Tunable Metamaterials for Antenna Applications</b>				5a. CONTRACT NUMBER	
				5b. GRANT NUMBER	
				5c. PROGRAM ELEMENT NUMBER	
6. AUTHOR(S) <b>Kamran Ghorbani</b>				5d. PROJECT NUMBER	
				5e. TASK NUMBER	
				5f. WORK UNIT NUMBER	
7. PERFORMING ORGANIZATION NAME(S) AND ADDRESS(ES) <b>RMIT University,GPO BOX 2476,Melbourne VIC 3000,Australia,NA,NA</b>				8. PERFORMING ORGANIZATION REPORT NUMBER <b>N/A</b>	
9. SPONSORING/MONITORING AGENCY NAME(S) AND ADDRESS(ES)				10. SPONSOR/MONITOR'S ACRONYM(S)	
				11. SPONSOR/MONITOR'S REPORT NUMBER(S)	
12. DISTRIBUTION/AVAILABILITY STATEMENT <b>Approved for public release; distribution unlimited.</b>					
13. SUPPLEMENTARY NOTES					
14. ABSTRACT <b>The increasing use of carbon fibre reinforced polymer CFRP in modern military aircraft together with the desire for a conformal load-bearing antenna structure, has since inspired the slotted waveguide antenna stiffened structure (SWASS) concept [1]. Conventional hat stiffened or blade stiffened aircraft panels fabricated in CFRP coincidentally exhibit internal dimensions that are typical of common military waveguide bands. By machining resonant slots at half-wavelength intervals in the outer skin of the stiffened panel, a SWA may be integrated into the aircraft structure to achieve potential weight and drag improvements over conventional aircraft antennas. These slots may be filled with a low-loss dielectric to retain the aerodynamic performance of the panel or with a high dielectric to reduce their physical dimensions.</b>					
15. SUBJECT TERMS					
16. SECURITY CLASSIFICATION OF:			17. LIMITATION OF ABSTRACT	18. NUMBER OF PAGES <b>7</b>	19a. NAME OF RESPONSIBLE PERSON
a. REPORT <b>unclassified</b>	b. ABSTRACT <b>unclassified</b>	c. THIS PAGE <b>unclassified</b>			

---

# 1 Introduction

The increasing use of carbon fibre reinforced polymer CFRP in modern military aircraft together with the desire for a conformal load-bearing antenna structure, has since inspired the slotted waveguide antenna stiffened structure (SWASS) concept [1]. Conventional hat stiffened or blade stiffened aircraft panels fabricated in CFRP coincidentally exhibit internal dimensions that are typical of common military waveguide bands. By machining resonant slots at half-wavelength intervals in the outer skin of the stiffened panel, a SWA may be integrated into the aircraft structure to achieve potential weight and drag improvements over conventional aircraft antennas. These slots may be filled with a low-loss dielectric to retain the aerodynamic performance of the panel or with a high dielectric to reduce their physical dimensions. Regardless, the structural impact of the slot is a significant concern for the SWASS concept [2].



Fig.1. SWASS concept.

This report divided into two sections: Section 2 presents a simple metamaterial inspired method employing a single split-ring resonator (SRR) to couple energy to the slot in a resonant SWA. This allows for a significant reduction in the slot length therefore overcoming the structural concerns of the SWASS concept without compromising the antenna performance. Section 3 explains the material analysis of BST varactors using the new sputterer so the varactors can be fabricated at RMIT university and utilised for the SRR.

## 2 SRR loaded sub-wavelength slot

The poor transmission of electromagnetic energy through a sub-wavelength aperture in an infinite metallic sheet is a classical problem that was first addressed by Bethe [3]. It remained a technical challenge until the experimental work of Ebbesen [4] and the theoretical analysis of Oliner and Jackson [5] established the role of surface plasmon polaritons in achieving enhanced transmission through a sub-wavelength aperture. However, the recent development of metamaterials inspired an alternative theoretical solution to the problem by Alu [6]. The practical issues regarding the experimental implementation of Alu's solution are discussed by Bilotti [7] who concludes with a resonant approach to the transmission enhancement problem.

This resonant approach to enhance the transmission employed a metamaterial constructed from magnetic inclusions such as the ubiquitous SRR. In [7], Bilotti demonstrates how such a metamaterial layer (with effective permeability of  $-1$ ) fabricated with transverse dimensions similar to the aperture size, may significantly enhance the transmitted power. However, a seconded enhancement peak in the transmitted spectrum was observed and attributed to the resonance of the SRR. This suggested the possibility of achieving enhanced transmission with the very simple addition of a well placed SRR behind the slot. Theoretical and

experimental work on this mechanism for enhanced transmission has since been reported in [8] and [9] with the possibility to tune the enhancement frequency reported in [10]. This method of achieving enhanced transmission from a sub-wavelength aperture may be applied to the SWASS concept to maximize the separation between the slots and therefore retain the mechanical performance of the CFRP. The proposed slot and SRR geometry is presented in Fig. 2.

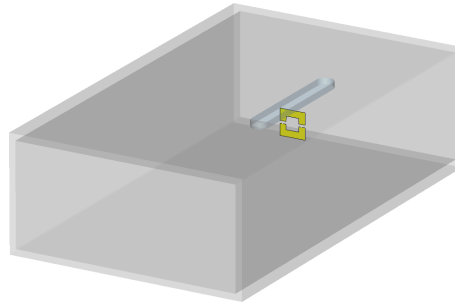


Fig. 2. SRR loaded slot in a rectangular waveguide. Waveguide ports are located at either end of the guide with lumped capacitances located in the SRR gap regions.

The SRR captures a portion of the magnetic flux circulating down the waveguide. The strong localized electric fields induced in the SRR couple to the slot to achieve a significant improvement in radiated power compared to the unloaded sub-wavelength length slot. For example, consider a square SRR with two splits, a mean ring dimension  $d = 3$  mm and ring width of 0.5 mm orientated in a WR-137 waveguide as illustrated in Fig. 2. Each gap in the SRR was loaded with a capacitance of 0.25 pF such that the SRR resonance occurred at 6.5 GHz. The slot offset from the broadwall centreline was set to 25 % of the broadwall dimension and the slot width was fixed at 2.6 mm.. The peak gain with and without the SRR loading may then be determined numerically using the frequency domain solver in CST. The slot length was varied to illustrate the advantage of the SRR loading in Fig 3.

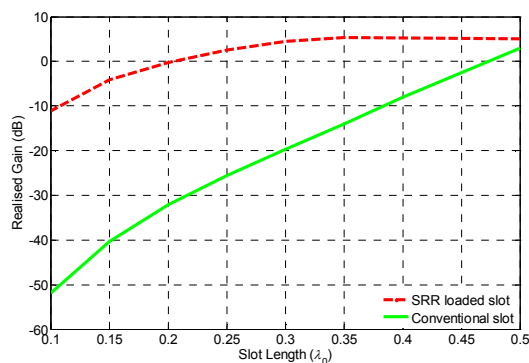


Fig. 3. Peak realized gain for a conventional single slot and for the SRR loaded slot at 6.5 GHz. The plane of the SRR is located at the centre of the slot.

Fig. 3 suggests a SWA with slot length of  $0.25 \lambda_0$  and SRR loading may exhibit comparable gain to a conventional SWA with resonant slot length of  $0.496 \lambda_0$  at 6.5 GHz in WR-137 waveguide. However, the SRR loaded SWA would provide greater mechanical stiffness over the conventional SWA.

### 3 Material analysis

Barium Strontium Titanate (BST) thin films were deposited on c-plane sapphire substrates using the new RF sputtering system with gas mixture of Ar/O<sub>2</sub> 9:1 O<sub>2</sub> and gas pressure at 5 mTorr. The RF power was 200 W, the deposition temperature was 700°C and the deposition time was 120 minutes. Material analyses were conducted as follows.

#### Analysis 1: X-Ray Diffraction (XRD)

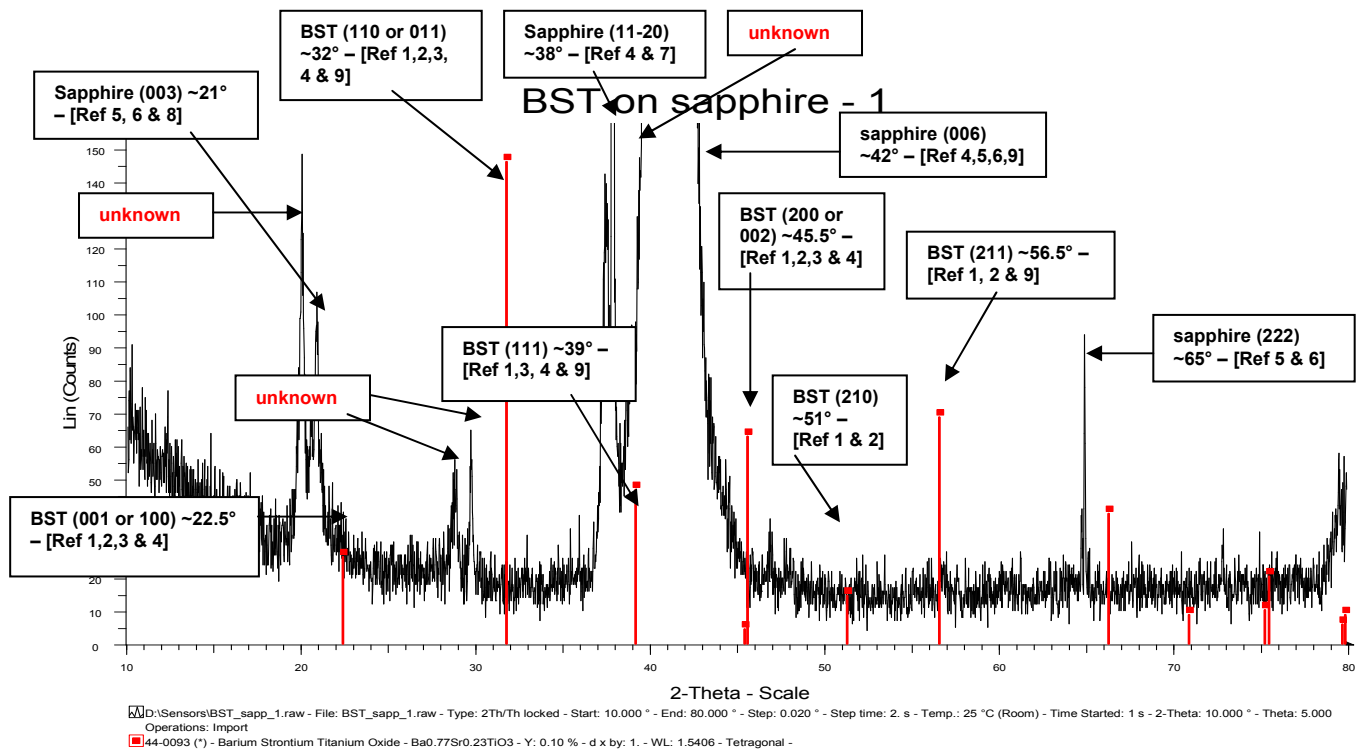


Fig.4. Sample 1 XRD pattern of BST film on sapphire substrate.

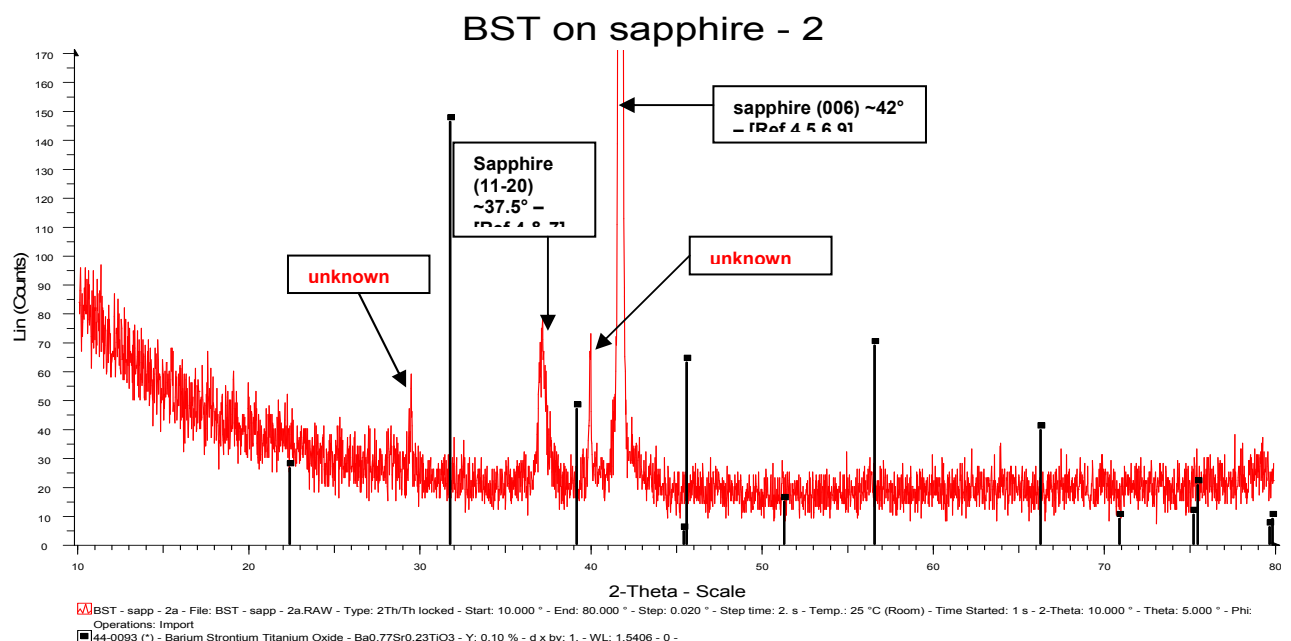


Fig. 5. Sample 2 XRD pattern of BST film on sapphire substrate.

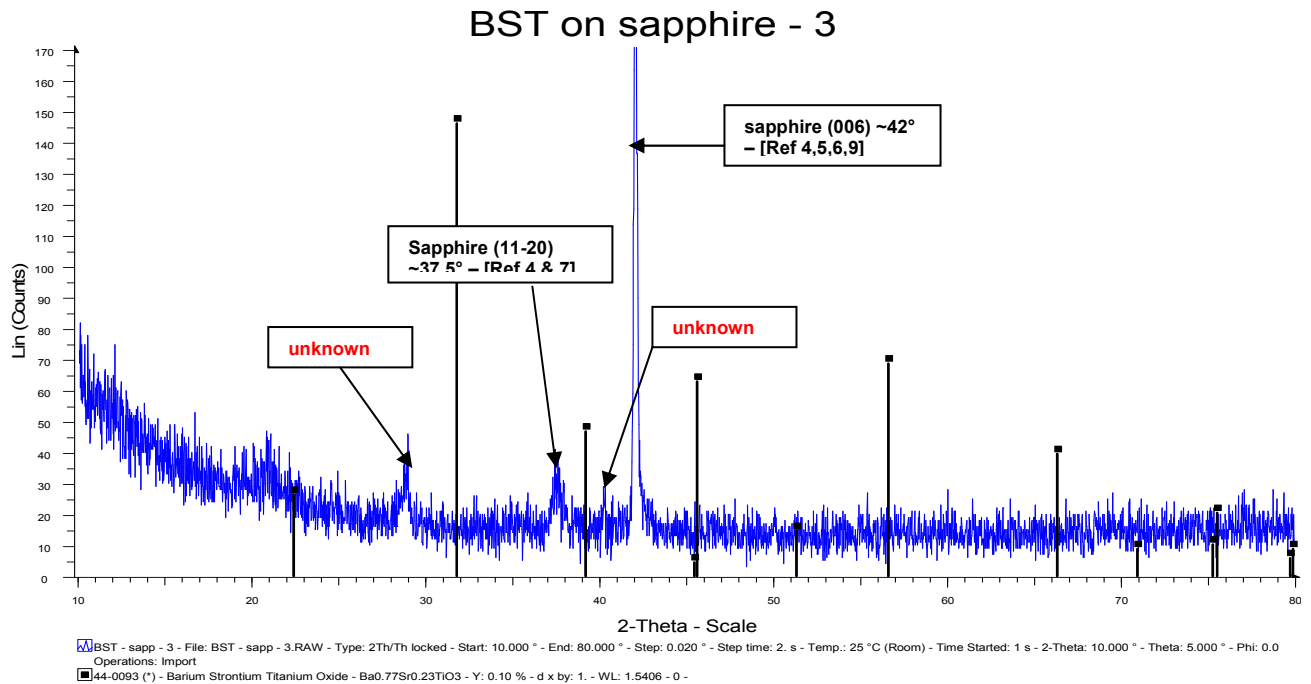


Fig. 6. Sample 3 XRD pattern of BST film deposited on sapphire substrate.

The results above show material analysis using powder X-ray diffraction (XRD). XRD provides information about the crystal structure of the BST films. As observed, the diffraction patterns of all samples contain some clearly resolved peaks, representative of crystalline material, and the baseline, although noisy, confirms that there is very little amorphous material present. The majority of the peaks have been assigned to the sapphire substrate, and to BST, but there are also some unknown peaks in the diffraction patterns of all samples, as seen in Fig.4. There are two unknown peaks which are consistent for all samples at  $\sim 29^\circ$  and  $\sim 40^\circ$ . The most intense unknown peak at  $\sim 40^\circ$  is being observed in Fig. 4. Unfortunately these peaks are not comparable to any standard BST patterns in the ICDD reference database or examples in published literature; hence they are unidentified at present. It is possible that the BST peaks may be shifted in position due to differences in chemical composition to that of the BST target.

### Analysis 2: X-Ray Photoelectron Spectroscopy (XPS)

Table 1. BST film compositions for all samples

	PP at. %			
	Ba3d5 Scan A	Sr3d5 Scan A	Ti2p3 Scan A	O1s Scan A + O1s Scan B
Sample 1	5.95	8.35	13.12	72.57
Sample 2	5.84	8.62	12.63	72.91
Sample 3	5.1	7.44	13.06	74.4

XPS provides information about the composition of the BST films. As observed, Table 1 indicates that the composition of the BST films is different from the BST target. The ideal composition of Ba<sub>0.6</sub> Sr<sub>0.4</sub> TiO<sub>3</sub> is 10 at.% Ba/Sr, 20 at.% Ti and 60 at.% O<sub>2</sub>. However, there are less at.% of Ba, Sr and Ti but more at.% of O<sub>2</sub> where the non-stoichiometry BST films obtained is Ba<sub>0.4</sub>Sr<sub>0.6</sub>TiO<sub>3</sub>.

### Analysis 3: X-Ray Diffraction (XRD) on Sample 2 – annealed in Argon for 1 hour at 700°C

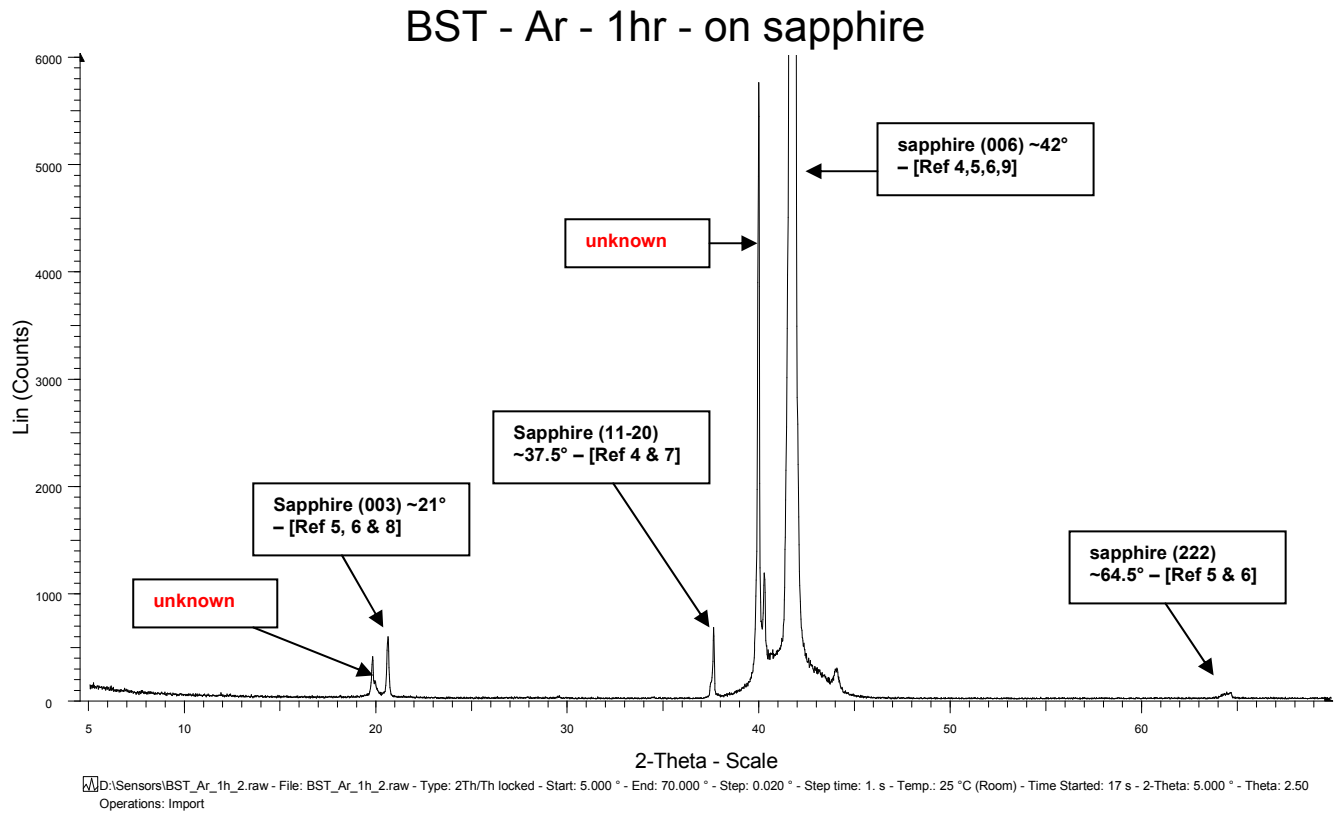


Fig. 7. Sample 2 XRD pattern of BST film deposited on sapphire substrate after one hour anneal in Argon at 700°C

Sample 2 from Fig. 5 was annealed in Argon at 700°C for one hour in a ceramic tube furnace to reduce the O<sub>2</sub> content within the sample. Post Ar treatment, the XRD pattern in Fig. 7 is more intense and more clearly resolved; indicating overall improved crystallinity of the sample. Also, two new strong peaks at ~20° and ~21° are observed in the pattern which were not present in Sample 2 before the annealing process, but were observed in Sample 1 from Fig. 4. The unknown peak at 40° is also more intense than before. These results indicate an improved crystallinity of the BST film, and possible improved orientation of the film.

## 4 Conclusions and recommendations

This report presented a simple metamaterial inspired method to achieve acceptable gain from a miniaturised slot. The results indicated that the gain of the slot antenna can be increased by 30 dB if the length of slot is  $0.2\lambda$ . In parallel with simulation of SRR loaded antenna, the fabrication of the BST varactors using sputterer and material properties were investigated. BST thin films with 50 nm thickness were deposited on sapphire substrate. XRD results of all three samples showed possible shifting of the BST peaks due to differences in chemical composition to that of the BST target. These were confirmed by the XPS results. XRD result of annealing process in Argon showed improved crystallinity and possible improved orientation of the BST film.

The next step is to fabricate the BST varactors and demonstrate the experimental results for the SRR loaded slot antenna. The integration of the SRR (using BST instead of

---

commercially available varactors) and the antenna to enhance the directivity will also be investigated.

## 5 References

- [1] P. Callus, *Novel concepts for conformal load-bearing antenna structure*. DSTO, 2008.
- [2] J. Sabat, *Structural response of slotted waveguide antenna stiffened structure components under compression*. AFIT, 2010.
- [3] H. A. Bethe, "Theory of Diffraction by Small Holes," vol. 66, no. 7, p. 163, 1944.
- [4] D. E. Grupp, H. J. Leze, T. Thio, and T. W. Ebbesen, "Beyond the Bethe Limit: Tunable Enhanced Light Transmission Through a Single Sub-Wavelength Aperture," *Advanced Materials*, vol. 11, no. 10, pp. 860-862, 1999.
- [5] A. A. Oliner and D. R. Jackson, "Leaky surface-plasmon theory for dramatically enhanced transmission through a subwavelength aperture, Part I: Basic features," in *IEEE Antennas and Propagation Society International Symposium*, vol. 2, pp. 1091–1094, 2003.
- [6] A. Alu, F. Bilotti, N. Engheta, and L. Vegni, "How metamaterials may significantly affect the wave transmission through a sub-wavelength hole in a flat perfectly conducting screen," in *IEE Seminar on Metamaterials for Microwave and (Sub) Millimetre Wave Applications: Photonic Bandgap and Double Negative Designs, Components and Experiments*, p. 11, 2003.
- [7] F. Bilotti, L. Scorrano, E. Ozbay, and L. Vegni, "Enhanced transmission through a sub-wavelength aperture: resonant approaches employing metamaterials," *Journal of Optics A: Pure and Applied Optics*, vol. 11, p. 114029, 2009.
- [8] A. O. Cakmak et al., "Enhanced transmission through a subwavelength aperture using metamaterials," *Applied Physics Letters*, vol. 95, no. 5, p. 052103, 2009.
- [9] K. Aydin et al., "Split-Ring-Resonator-Coupled Enhanced Transmission through a Single Subwavelength Aperture," *Physical Review Letters*, vol. 102, no. 1, p. 013904, Jan. 2009.
- [10] C. Huang, Z. Zhao, and X. Luo, "Tuning enhanced transmission frequency through a subwavelength aperture with active split ring resonator," presented at the 5th International Symposium on Advanced Optical Manufacturing and Testing Technologies: Smart Structures and Materials in Manufacturing and Testing, Dalian, China, pp. 765902-765902-5, 2010.